*Journal of Applied Mechanics and Technical Physics, Vol. 41, No. 3, 2000*

# STABILITY OF NON-NEWTONIAN FLUID FLOWS

**L. A. Spodareva**

UDC 532.536

*The stability of non-Newtonian fluid films moving on inclined planes is studied within the framework of the two-parameter Ostwald–de Waele model taking into account surface tension and van der Waals forces. The problem is solved analytically in the linear formulation, and the evolution of finite-amplitude perturbations is determined numerically.*

Non-Newtonian fluids are characterized by a nonlinear relationship between the shear stress and the shear velocity of the flow. These fluids are often encountered in nature and industrial technologies (volcanic lava, mudflows, oil, plastics, oil-based paints, and polymer solutions and melts).

A model that offers a satisfactory description of the motion of anomalously viscous non-Newtonian fluids is the Ostwald–de Waele model with a power-law relationship between the shear stress and the shear velocity (see, e.g., [1]). This model contains the dynamic viscosity $\eta_0$ and the exponent $n$ characterizing the non-Newtonian behavior of the fluid: the more the value of $n$ differs from unity ($n = 1$ corresponds to the Newtonian fluid), the more distinctly the anomalously viscous properties are manifested. Depending on the exponent, non-Newtonian fluids are classified into pseudoplastic ones ($n < 1$), for example, petroleum and some oils ($n \simeq 0.8$), and dilatant fluids ($n > 1$), for example, saccharified honey ($n > 2$) [1–3]. A dry granular medium in the inertial regime can be considered as a dilatant fluid with $n = 2$ [4–6], since the shear stress in such a medium is proportional to the shear velocity squared.

In the present work, we consider the stability of layers of incompressible non-Newtonian fluids moving over a rough inclined plane to perturbations of small and finite amplitudes with account of surface tension. The analysis is performed on the basis of the equations of mass and momentum balance averaged over the layer thickness, which are supplemented by the Ostwald–de Waele equation of state. The corresponding linear analysis of stability with ignored surface tension was performed in [7, 8], and Hwang et al. [9] presented a brief linear analysis with account of surface tension for small deviations of the fluid properties from Newtonian ones ($n = 1 \pm \delta$, where $\delta \ll 1$). Berezin et al. [8] also gave some results of a numerical study of the evolution of localized finite-amplitude perturbations.

Assuming, as in [7, 8], that the characteristic thickness of a fluid layer $H_0$ is much smaller than the characteristic linear size $L_0$ ($\varepsilon \equiv H_0/L_0 \ll 1$), we write the initial equations and boundary conditions taking into account surface tension on the solid plane and free surface:

$$u_t + uu_x + vu_y = -(p + \varphi)_x/\rho + g\sin\beta + \nu_n(|u_y|^{n-1}u_y)_y,$$
$$p_y = -\rho g\cos\beta, \quad u_x + v_y = 0; \tag{1}$$

$$u = v = 0 \quad \text{for} \quad y = 0;$$
$$p = -\alpha H_{xx}, \quad u_y = 0, \quad H_t + uH_x = v \quad \text{for} \quad y = H(x,t). \tag{2}$$

Novosibirsk Military Institute, Novosibirsk 630117. Translated from Prikladnaya Mekhanika i Tekhnicheskaya Fizika, Vol. 41, No. 3, pp. 75–80, May–June, 2000. Original article submitted June 17, 1999; revision submitted September 7, 1999.

 

Here $x$ is the coordinate along the inclined plane, $y$ is the coordinate perpendicular to the latter, $t$ is the time, $\rho$ is the fluid density, $g$ is the acceleration of gravity, $p$ is the pressure, $u$ and $v$ are the velocity components, $\beta$ is the angle with the horizontal plane, $\nu_n$ [$\mathrm{m}^2 \cdot \mathrm{sec}^{n-2}$] is the kinematic viscosity of a non-Newtonian fluid with an exponent $n$, $\varphi = A_H/H^3$ is the potential of long-range molecular van der Waals forces, and $A_H$ [J] is the Hamaker constant (see, e.g., [10, 11]).

Following [12, 13], we average Eqs. (1) over the layer thickness by integrating them over the $y$ coordinate from the bottom of the layer $y = 0$ to the free surface $y = H(x,t)$ using the boundary conditions (2). As a result, we obtain the following equations in dimensionless variables:

$$H_t + Q_x = 0,$$
$$Q_t + \frac{4n+2}{3n+2}\Big(\frac{Q^2}{H}\Big)_x = \frac{1}{\varepsilon \mathrm{O}_n}\Big(\frac{2n+1}{n}\Big)^n \Big\{\Big[1 - \varepsilon H_x \cot\beta\Big(1 - \frac{3A_0}{H^4\cos\beta}\Big)\Big]H - \frac{Q^n}{H^{2n}}\Big\} + \varepsilon^2 \mathrm{We}_n H H_{xxx}. \tag{3}$$

Here $Q$ is the volume discharge of the fluid and $\mathrm{O}_n$ is the Ostwald number. The following scales were used to pass to dimensionless variables: characteristic distances along and across the layer ($L_0$ and $H_0$, respectively), $\varepsilon = H_0/L_0 \ll 1$, the time $t_0 = L_0/u_0$, and the longitudinal velocity $u_0 = Q_0/H_0$. The discharge scale is

$$Q_0 = \Big(\frac{g\sin\alpha}{\nu_n}\Big)^{1/n} \frac{n}{2n+1} H_0^{(2n+1)/n}.$$

The dimensionless parameter $\mathrm{O}_n = H_0^{2n-2}Q_0^{2-n}/\nu_n = H_0^n u_0^{2-n}/\nu_n$, which was called the Ostwald number in [8], is an analog of the Reynolds number for non-Newtonian media that obey the power law. Another dimensionless parameter $\mathrm{We}_n = \sigma H_0/(\rho Q_0^2) = \sigma/(\rho u_0^2 H_0)$ is the Weber number for a non-Newtonian fluid; $A_0 = A_H/(\rho g H_0^4)$ and $\sigma$ is the surface tension.

As in [7–9], we linearize system (3) relative to small perturbations of a moving homogeneous layer of constant thickness assuming that $H = 1 + h$ and $Q = 1 + q$ ($h, q \ll 1$). Representing the solution of the resultant system of two linear equations in the form of periodic waves $h, q \sim \exp(i(kx - \omega t))$, we obtain the dispersion equation

$$\omega^2 - (2ak - ib)\omega + ck^2 - ifk - \varepsilon^2 \mathrm{We}_n k^4 = 0, \tag{4}$$

where $\omega$ is the complex frequency, $k$ is the real wavenumber of small perturbations, $a = (4n+2)/(3n+2)$, $b = ((2n+1)/n)^n n/(\varepsilon \mathrm{O}_n)$, $c = a - ((2n+1)/n)^n(1 - 3A_0/\cos\beta)\cot\beta/\mathrm{O}_n$, and $f = b(2n+1)/n$. We write the complex frequency in the form $\omega = \omega_r + i\gamma$, where $\omega_r$ is the real frequency and $\gamma$ is the growth rate, and introduce the phase velocity of perturbations $v = \omega_r/k$. Substituting these formulas into (4) and separating the real and imaginary parts, we obtain

$$\gamma = b(v_0 - v)/(2(v - a)): \tag{5}$$

$$\varepsilon^2 \mathrm{We}_n k^4 - (v^2 - 2av + c)k^2 - b^2(v - v_0)(v + v_0 - 2a)/(4(v-a)^2) = 0, \tag{6}$$

where $v_0 = f/b$. With accuracy to notation, Eqs. (5) and (6) coincide with the corresponding equations for the cases $\mathrm{We}_n = 0$ [7, 8] and $\mathrm{We}_n \neq 0$ [9]. We also note that Eqs. (5) and (6) are transformed to those given in [12] in the special case of the Newtonian fluid ($n = 1$).

It follows from (5) that the growth rate $\gamma$ is positive for $v < v_0$ and negative for $v > v_0$. Thus, the motion of a homogeneous layer under consideration is unstable to small periodic perturbations with a phase velocity $v < v_0$ and stable to small perturbations that have a phase velocity $v > v_0$. This critical phase velocity is equal to $v_0 = (2n+1)/n$; for small values of $n$ (strongly pseudoplastic fluids), we have $v_0 \sim n^{-1}$, and for $n \to \infty$ (strongly dilatant fluids), we obtain $v_0 = 2$. For the Newtonian fluid, we have $v_0 = 3$.

Relation (6) is a biquadratic equation for the wavenumber, and the expression for the wavenumber squared has the form

$$k^2 = \frac{(v - v_1)(v - v_2)}{2\varepsilon^2 \mathrm{We}_n}\Big\{1 \pm \Big[1 - \frac{\varepsilon^2 \mathrm{We}_n b^2 (v_0 - v)(v_0 + v - 2a)}{(v-a)^2(v-v_1)^2(v-v_2)^2}\Big]^{1/2}\Big\}, \tag{7}$$

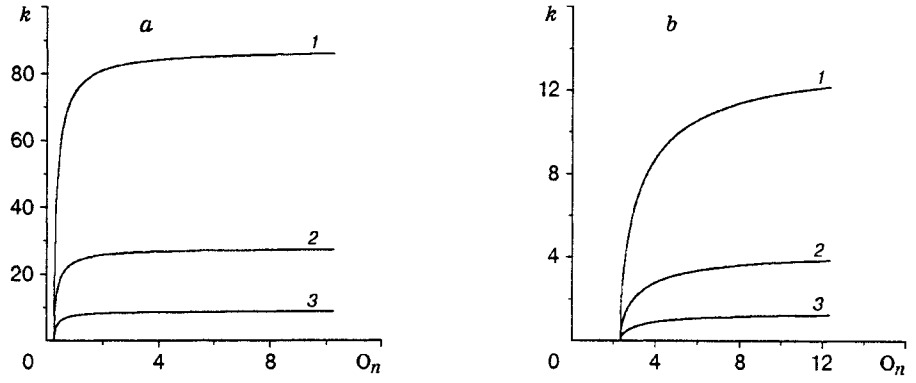


Fig. 1. Neutral curves of stability: (a) solution of napalm in kerosene ($n = 0.52$ and $O_n^* = 0.27$): We = 0.1 (curve 1), 1 (curve 2), and 10 (curve 3): (b) lime–water mixture ($n = 1.47$ and $O_n^* = 2.33$): We = 1 (curve 1), 10 (curve 2), and 100 (curve 3).

where $v_1 = a + (a^2 - c)^{1/2}$ and $v_2 = a - (a^2 - c)^{1/2}$. The growth rate $\gamma$ vanishes for $v = v_0$. This happens for two values of the wavenumber: $k^2 = 0$ and $k^2 \equiv k_*^2 = (v_0 - v_1)(v_0 - v_2)/(\varepsilon^2 \mathrm{We}_n)$. Substituting the values of $v_0$, $v_1$, and $v_2$, we find the boundary wavenumber squared:

$$k_*^2 = \frac{2n+1}{\varepsilon^2 \mathrm{We}_n n^2}\left[1 - (2n+1)^{n-1} n^{2-n}\left(1 - \frac{3A_0}{\cos\beta}\right)\frac{\cot\beta}{\mathrm{O}_n}\right]. \tag{8}$$

It follows from this formula and above considerations that the flow under study is stable ($\gamma \leqslant 0$) for $\mathrm{O}_n \leqslant \mathrm{O}_n^*$, where $\mathrm{O}_n^* = (2n+1)^{n-1} n^{2-n}(1 - 3A_0/\cos\beta)\cot\beta$ is the critical Ostwald number. In the case of fluid motion over a vertical wall ($\beta = 90°$), the critical Ostwald number is equal to zero for $A_0 = 0$ and negative for $A_0 \neq 0$; therefore, perturbations are unstable for all Ostwald numbers. Taking into account van der Waals forces ($A_0 \neq 0$) leads to a decrease in $\mathrm{O}_n^2$. Nevertheless, since the Hamaker constant is small (for example, for water films we have $A_H \approx 10^{-20}$ J), the influence of this effect is significant only for ultrathin films of thickness of the order of $10^{-7}$ m. If the Ostwald number is greater than the critical value, there exists a finite region of wavenumbers $\Delta k = 0$–$k_*$, wherein small perturbations are unstable (the growth rate is positive). If the surface tension is ignored, the region of unstable wavenumbers is unbounded ($k \to \infty$) (8). The surface tension stabilizes small-scale perturbations, making the region of unstable wavenumbers finite ($k_* \sim \mathrm{We}_n^{1/2}$).

For small deviations of the Ostwald number from the critical value, when $\mathrm{O}_n = \mathrm{O}_n^*(1+\delta)$, where $\delta \ll 1$, we have $k_*^2 = (\varepsilon^2 \mathrm{We}_n)^{-1}\delta(2n+1)/n^2$ from [8]. Hence, for fluids with small exponents, the boundary value of the unstable wavenumber is $k_* \sim n^{-1}$, and in the case of fluids with high exponents, we have $k_* \sim n^{-1/2}$. For fixed values of the Weber number and Ostwald numbers other than the critical one, the boundary wavenumber decreases monotonically as we pass from pseudoplastic media to dilatant ones. From formula (6), we obtain the equation of the neutral curve $\mathrm{O}_n = \mathrm{O}_n(k)$ separating the regions of stability and instability:

$$\mathrm{O}_n = \mathrm{O}_n^*/(1 - \varepsilon^2 \mathrm{We}_n n^2 k^2/(2n+1)).$$

Two fluids (pseudoplastic and dilatant) were chosen for calculations. Their parameters can be found in [1]: napalm solution in kerosene ($n = 0.52$, $\nu = 5.35 \cdot 10^{-3}$ m$^2 \cdot$ sec$^{n-2}$, $\sigma = 0.026$ N/m, and $\rho = 800$ kg/m$^3$) and lime/water mixture ($n = 1.47$, $\nu = 2.5 \cdot 10^{-7}$ m$^2 \cdot$ sec$^{n-2}$, $\sigma = 0.076$ N/m, and $\rho = 1000$ kg/m$^3$). In all calculations, we had $\varepsilon = 0.1$ and $\beta = 45°$. The neutral curves for various Weber numbers are shown in Fig. 1. Regions above and to the left of these neutral curves correspond to stability, and those below and to the right of the neutral curves correspond to instability.

If the power-law functions are inspected from the mathematical point of view, the parameters $n$, $\mathrm{O}_n$, and $\mathrm{We}_n$ can be chosen independently of each other. If the calculations are made for particular fluids, these parameters cannot be chosen independently. Indeed, the Ostwald and Weber numbers depend on the discharge $Q_0$ whose substitution into the corresponding formulas yields

$$\mathrm{O}_n = (g\sin\beta)^{(2-n)/n} n^{2-n}(2n+1)^{n-2}\nu_n^{-2/n} H_0^{(n+2)/n},$$

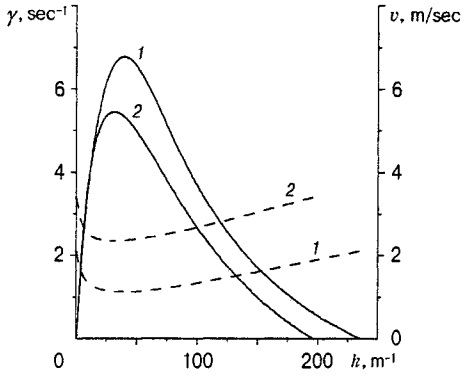


Fig. 2. Growth rates (solid curves) and phase velocities (dashed curves) versus the wavenumber: $n = 0.52$, $O_n = 7.2$, and $We = 1$ (curves 1) and $n = 1.47$, $O_n = 488$, and $We = 11.9$ (curves 2).

$$We_n = (\sigma/\rho)(g \sin\beta)^{-2/n} n^{-2}(2n+1)^2 \nu_n^{2/n} H_0^{-(3n+2)/n}.$$

The fluid parameters $n$, $\nu_n$, and $\sigma/\rho$ and the angle of inclination $\beta$ given, the only quantity determining the Ostwald and Weber numbers is the unperturbed thickness of the layer $H_0$ whose variation leads to simultaneous variation of these numbers; the greater this thickness, the greater the Ostwald number and the smaller the Weber number, and vice versa.

Figure 2 shows the growth rates and phase velocities of small perturbations versus the wavenumber.

The evolution of finite-amplitude perturbations was studied numerically. For a numerical solution of system (3) with ignored surface tension, Berezin et al. [8] used an explicit finite-difference scheme in which the mass and momentum fluxes were approximated by one-sided differences in accordance with the flow direction, and the term $HH_x$ proportional to the pressure gradient was approximated by the central difference. This scheme possesses conventional stability; the ratio of the steps $\delta t/\delta x$ necessary for stability was chosen by additional calculations. Taking into account surface tension increases the order of the highest derivative relative to the coordinate up to three. This scheme supplemented by a symmetric finite difference for approximation of the third derivative was used to solve system (3):

$$H1_i = H_i - \frac{\delta t}{\delta x}(u_{i+0.5}H_i - u_{i-0.5}H_{i-1}),$$

$$Q1_i = Q_i - a_n \frac{\delta t}{\delta x}(u_{i+0.5}u_i H_i - u_{i-0\,5}u_{i-1}H_{i-1}) - \varepsilon b_n \cot\beta \frac{\delta t}{2\delta x} H_i(H_{i+1} - H_{i-1})$$

$$+ b_n \delta t\left[H_i - \frac{Q_i^n}{H_i^{2n}}\right] + \varepsilon^2 We_n \frac{\delta t}{2\delta x^3} H_i(H_{i+2} - 2H_{i+1} + 2H_{i-1} - H_{i-2}).$$

Here $H1_i \equiv H_i^{m+1}$, $Q1_i \equiv Q_i^{m+1}$, $H_i \equiv H_i^m$, $Q_i \equiv Q_i^m$; $t^{m+1} = (m+1)\delta t$, $t^m = m\delta t$, $u_{i+0.5} = (u_i + u_{i+1})/2$, $u_{i-0.5} = (u_i + u_{i-1})/2$, $a_n = (4n+2)/(3n+2)$, and $b_n = (\varepsilon O_n)^{-1}((2n+1)/n)^n$. The scheme is convenient for implementation, and its conventional stability, which requires choosing $\delta t < \delta x^3$, is not a great restriction because of the one-dimensionality of the problem. The initial localized perturbation was chosen in the form of an isosceles triangle with a height of 0.1 of the thickness of an unperturbed fluid layer. The free-stream conditions $H = 1$ and $H_x = H_{xx} = 0$ for $x = 0$ and $x = x_{max}$ were used as the boundary conditions. The use of these boundary conditions implies that the numerical solution is performed as long as this perturbation is rather far from the boundaries of the computational domain (this condition is defined in the algorithm).

Figure 3a shows the profile of the free surface of a layer of a pseudoplastic fluid ($n = 0.52$) moving over an inclined plane at the times $t = 0$ and 10 (in dimensionless units) after sudden liberation of the initial bubble for $O_n = 7.2$ and $We = 0$, which corresponds to the absence of surface tension. Since the Ostwald

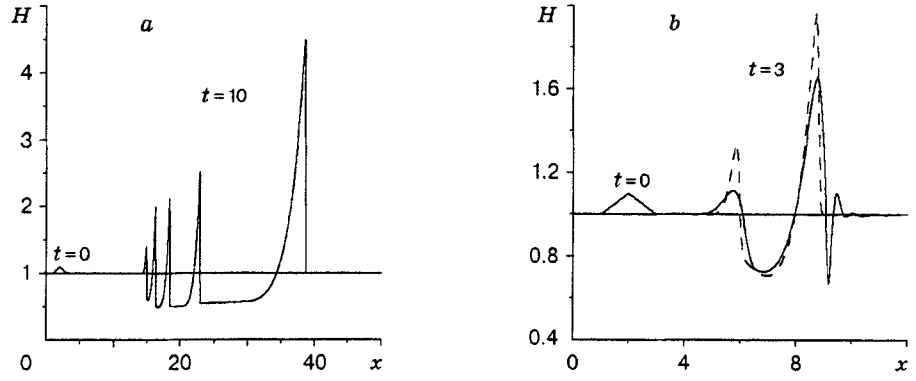


Fig. 3. Profiles of the free surface of a liquid layer for $n = 0.52$ and $O_n = 7.2$: (a) $t = 0$ and 10 and We = 0; (b) $t = 0$ and 3 and We = 1 (solid curve) and We = 0 (dashed curve).

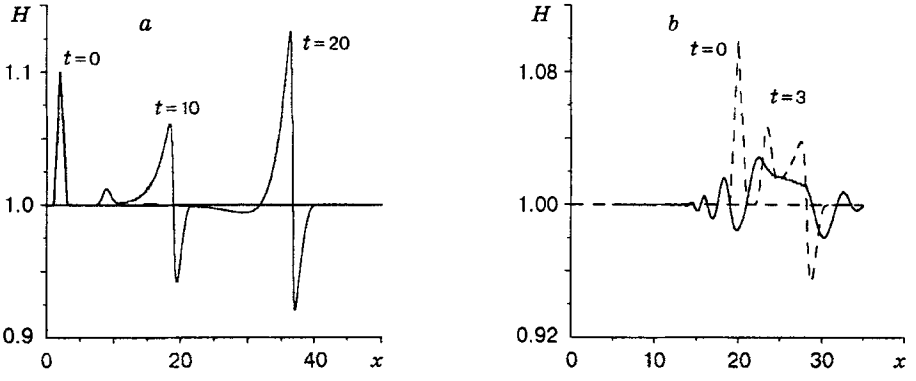


Fig. 4. Profiles of the free surface of a liquid layer for $n = 1.47$ and $O_n = 488$: (a) $t = 0$, 10, and 20 and We = 0; (b) $t = 0$ and 3 and We = 11.9 (solid curve) and 0 (dashed curve).

number is greater than the critical value 0.23, the initial perturbation of a triangular form is unstable; a wave structure consisting of a number of compression teeth with sharp leading edges arises with time. Gradually, the first tooth moves away from the rest of the teeth, and a region where the free surface is lower than the unperturbed level appears between the first and the next tooth. Such a structure consisting of a shock with a sharp leading front and subsequent rarefaction acquires a form similar to steady solutions analyzed by Ng and Mei [7]. Thus, a typical feature of each part of the overall wave structure is a very narrow front, a smooth decrease in amplitude when moving to the region of lower values of the $x$ coordinate, and a rather extended region between the subsequent shocks where $H < 1$.

Figure 3b shows the calculation results for the free-surface profile at the times $t = 0$ and 3 for $O_n = 7.2$, where the effect of surface tension is taken into account (solid curve) or not (dashed curve). The amplitudes of shocks decrease in the presence of surface tension, and an oscillator precursor moving ahead of the disturbance front appears on the free-surface profile. This phenomenon can be explained by dispersion of low-amplitude modes. Thus, though the presence of surface tension does not change the critical Ostwald number, its action is manifested in the decrease in amplitude and dispersion smearing of the profile.

Figure 4a and b shows the profiles of the free surface of a layer of a dilatant fluid ($n = 1.47$) without and with account of the surface tension forces, respectively. The surface tension leads to formation of a typical dispersion structure with oscillations both ahead of and behind the main front (Fig. 4b).

The author is grateful to Yu. A. Berezin for useful discussions.

## REFERENCES


1. Z. P. Shul'man and B. M. Berkovskii, *Boundary Layer of Non-Newtonian Fluids* [in Russian], Nauka Tekhnika, Minsk (1966).
2. R. B. Bird, R. C. Armstrong, and O. Hassager, *Dynamics of Polymeric Liquids*, Vol. 1, John Wiley and Sons, New York (1977).
3. F. R. Eirich, *Rheology*, Vol. 4, Academic Press, New York (1967).
4. R. A. Bagnold, "Experiments on a gravity free dispersion of large solid spheres in a Newtonian fluid under shear," *Proc. Roy. Soc. London*, **A225**, 49–63 (1954).
5. Yu. A. Berezin, K. Hutter, and L. A. Spodareva, "Stability properties of shallow granular flows," *Int. J. Non-Linear Mech.*, **33**, No. 4, 647–658 (1998).
6. Yu. A. Berezin and L. A. Spodareva, "Analysis of stability of a thin layer of granular material moving on an inclined plane," *Prikl. Mekh. Tekh. Fiz.*, **39**, No. 6, 113–117 (1998).
7. C. Ng and C. C. Mei, "Roll waves on a shallow layer of mud modelled as a power-law fluid," *J. Fluid Mech.*, **263**, 151–183 (1994).
8. Yu. A. Berezin, K. Hutter, and L. A. Spodareva, "Stability analysis of gravity driven shear flows with free surface for power-law fluids," *Arch. Appl. Mech.*, **68**, 169–178 (1998).
9. C. Hwang, J. Chen, J. Wang, and J. Lin, "Linear stability of power-law liquid film flows down an inclined plane," *J. Phys., D, Appl. Phys.*, **27**, 2297–2301 (1994).
10. T. Erneux and S. H. Davis, "Nonlinear rupture of free films," *Phys. Fluids*, **A5**, No. 5, 1117–1122 (1993).
11. A. de Witt, D. Gallez, and C. I. Christov, "Nonlinear evolution equations for thin liquid films with insoluble surfactants," *Phys. Fluids*, **6**, No. 10, 3256–3266 (1994).
12. S. V. Alekseenko, B. E. Nakoryakov, and B. G. Pokusaev, "Wave formation in a flow of a liquid film over a vertical wall," *Prikl. Mekh. Tekh. Fiz.*, No. 6, 77–87 (1979).
13. S. V. Alekseenko, B. E. Nakoryakov, and B. G. Pokusaev, *Wave Flow of Liquid Films* [in Russian], Nauka, Novosibirsk (1992).